

TECHNICAL RESEARCH REPORT

Analysis and Control of Period Doubling Bifurcation in Buck Converters Using Harmonic Balance

by C.-C. Fang, E.H. Abed

T.R. 98-50



ISR develops, applies and teaches advanced methodologies of design and analysis to solve complex, hierarchical, heterogeneous and dynamic problems of engineering technology and systems for industry and government.

ISR is a permanent institute of the University of Maryland, within the Glenn L. Martin Institute of Technology/A. James Clark School of Engineering. It is a National Science Foundation Engineering Research Center.

Web site <http://www.isr.umd.edu>

Analysis and Control of Period Doubling Bifurcation in Buck Converters Using Harmonic Balance

Chung-Chieh Fang and Eyad H. Abed*
Department of Electrical Engineering
and the Institute for Systems Research
University of Maryland
College Park, MD 20742 USA
ccfang@isr.umd.edu, abed@isr.umd.edu

Manuscript: Sept. 20, 1998

Abstract

Period doubling bifurcation in buck converters is studied by using the harmonic balance method. A simple dynamic model of a buck converter in continuous conduction mode under voltage mode or current mode control is derived. This model consists of the feedback connection of a linear system and a nonlinear one. An exact harmonic balance analysis is used to obtain a necessary and sufficient condition for a period doubling bifurcation to occur. If such a bifurcation occurs, the analysis also provides information on its exact location. Using the condition for bifurcation, a feedforward control is designed that eliminates a period doubling bifurcation. This results in a wider range of allowed source voltage, and also in improved output voltage regulation.

1 Introduction

Several authors have investigated the occurrence of period doubling bifurcation in DC-DC converters [1, 2, 3, 4]. A period doubling bifurcation entails loss of stability of the nominal operating condition, and as such is undesirable. Moreover, a period doubling route to chaos could be signaled by such a bifurcation, eroding the performance of the circuit. This has led to preliminary investigations of methods for prevention of period doubling bifurcations in DC-DC converters [5, 6].

*Corresponding author

In this work, analysis and control of period doubling bifurcation of a buck converter in continuous-conduction mode are considered. A continuous-time feedback system model is used as the basis for a harmonic balance analysis of period doubling bifurcation as well as control design for preventing the onset of period doubling. The model separates the nonlinear switching action of the converter from the linear filtering action. Because the model resolves dynamics within switching intervals, it is more accurate than the traditional averaged models [7]. In addition, the model proposed here is valid both for current mode control and voltage mode control.

An exact harmonic balance analysis is used to obtain a necessary and sufficient condition for a period doubling bifurcation to occur. If such a bifurcation occurs, the analysis also provides information on its exact location. Using the condition for bifurcation, a feedforward control is designed that eliminates a period doubling bifurcation. This results in a wider range of allowed source voltage, and also in improved output voltage regulation.

Harmonic balance analysis of period doubling bifurcations has been pursued for general nonlinear systems in [8, 9, 10]. Unlike the approximate but general treatments given in [8, 9, 10], in this paper an exact harmonic balance analysis is performed. This is made possible by the special structure of the buck converter model. For other converters, a more typical approximate harmonic balance analysis can be performed.

It is noteworthy that harmonic balance analysis has previously been applied in power electronics in the context of small-signal modeling [11, 12].

The remainder of the paper is organized as follows. In Section 2, a simple dynamic model for the buck converter in continuous conduction mode under voltage mode or current mode control is proposed. In Section 3, the harmonic balance method is used to study period doubling bifurcation for the buck converter. In Section 4, feedforward control is used to eliminate period doubling bifurcation in the buck converter. In Section 5, an illustrative example is given. Conclusions are collected in Section 6.

2 Simple Dynamic Model for the Buck Converter in Continuous Conduction Mode Under Voltage Mode Control or Current Mode Control

A buck converter under voltage mode control is shown in Fig. 1. The source voltage and output voltage are assumed constant, and are denoted by V_s and V_o , respectively. The voltage across the diode is denoted by v_d . Output signal of the error amplifier is denoted by $y(t)$. The ramp signal, denoted by $h(t)$, is a T -periodic function with $h(0) = V_l$ and $h(T) = V_h$. The switching period is T , the switching frequency is $f_s = 1/T$, and the angular switching frequency is $\omega_s = 2\pi f_s$.

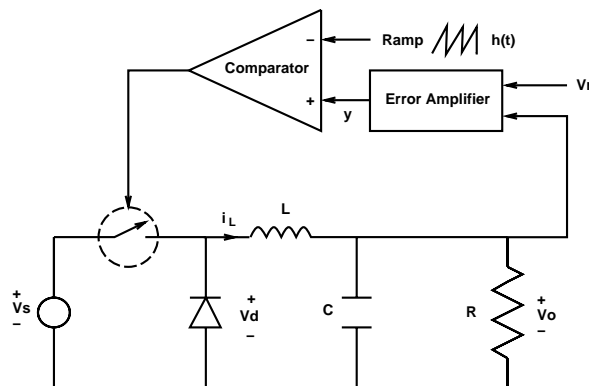


Figure 1: Buck converter under voltage mode control

The switching operation in continuous conduction mode (with lead-edge modulation) is as follows. When $y(t) < h(t)$, the switch is on, the diode is off, and $v_d = V_s$. When $y(t) \geq h(t)$, the switch is off, the diode is on, and $v_d = 0$. Thus the signal $v_d(t)$ is a square wave, and the switch/diode combination can be modeled as a controlled square wave generator.

The output filter (L and C) and the load (R) in Fig. 1 form a low-pass filter with transfer function

$$G_1(s) = \frac{v_o(s)}{v_d(s)} = \frac{1}{LCs^2 + \frac{L}{R}s + 1} \quad (1)$$

For a buck converter with a more complex power stage (for example, with a second output filter, or with an equivalent series resistance in parallel with the capacitor C), the model remains valid,

but with a more complex transfer function $G_1(s)$.

Generally the error amplifier is linear and is driven by the signals V_r and v_o . Its output can be represented as

$$y(t) = gV_r + (g_2 \circ v_o)(t) \quad (2)$$

where g is a gain constant and g_2 is an impulse response function. Denote the transfer function associated with g_2 by G_2 . Since G_2 depends on the control scheme, no further restriction is placed on it.

Thus the buck converter in continuous conduction mode can be modeled as a system block diagram as shown in Fig. 2.

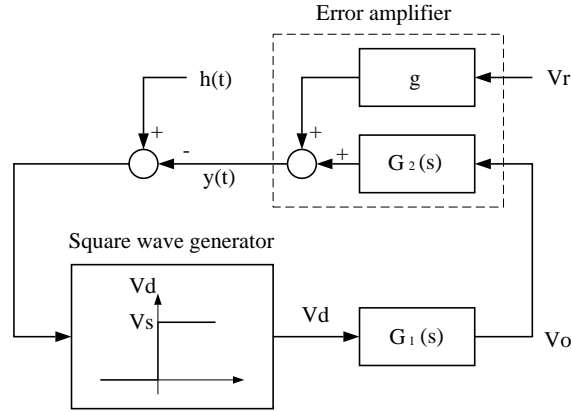


Figure 2: Dynamic model of buck converter in continuous conduction mode under voltage mode control

For a buck converter under current mode control as depicted in Fig. 3, the switch operation is different from that in voltage mode control. In current mode control, the switch turns on at each clock pulse and turns off at instants when $y(t) = h(t)$. The switch/diode combination can also be modeled as a controlled square wave generator. Therefore, a buck converter under current mode control can be modeled by the system block diagram in Fig. 4, where a linear transfer function

$$G_i(s) = \frac{R_s i_L(s)}{v_d(s)} = \frac{R_s(RCs + 1)}{RLCs^2 + Ls + R} \quad (3)$$

is placed in the current feedback path. The remaining notation is the same as for the case of voltage

mode control.

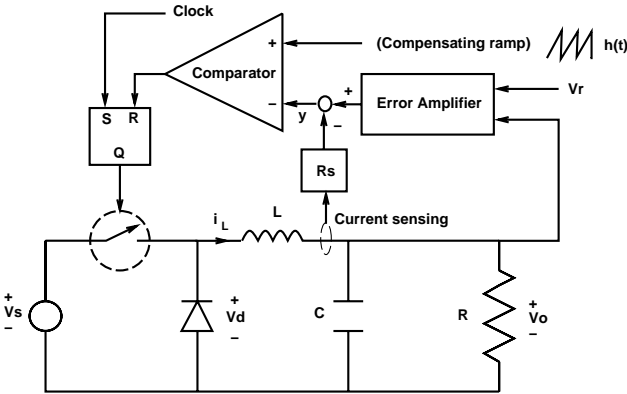


Figure 3: Buck converter under current mode control

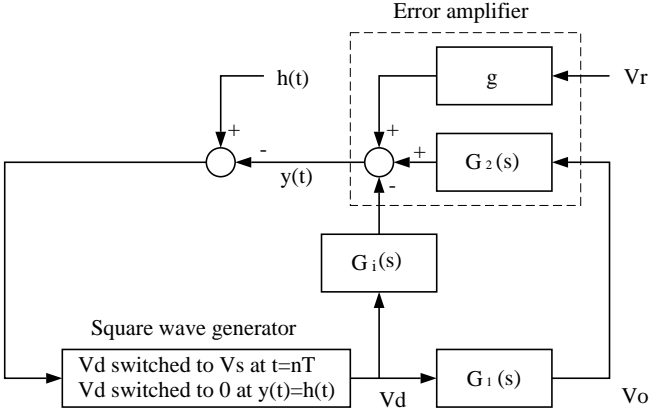


Figure 4: Dynamic model of buck converter under current mode control in continuous conduction mode

Despite the differences in switching operation in voltage mode control and current mode control, they can be modeled in a unified setting. Both Fig. 2 and Fig. 4 can be further simplified as Fig. 5, where $G(s) = G_1(s)G_2(s)$ in the case of voltage mode control and $G(s) = G_1(s)G_2(s) - G_i(s)$ in the case of current mode control. For either case, the controlled buck converter is a combination of a linear system $G(s)$ and a nonlinear one (a controlled square wave generator).

In the remainder of the paper, only voltage mode control is considered. The results extend readily to the case of current mode control.

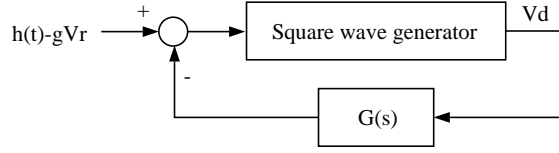


Figure 5: Simplified dynamic model of controlled buck converter in continuous conduction mode

3 Determination of Period Doubling Bifurcation Point Using Harmonic Balance

Assume the nominal operating condition is a T -periodic solution (in period-one mode). Representative waveforms for $y(t)$ and $v_d(t)$ are shown in Fig. 6. At the switching time $t = d$,

$$y(d) = h(d) \quad (4)$$

When period doubling bifurcation occurs, a $2T$ -periodic solution arises from the original T -periodic solution. Representative waveforms for $y(t)$ and $v_d(t)$ for this $2T$ -periodic solution are depicted in Fig. 7. Switchings occur at $t = d - \delta$ and at $T + d + \delta$, where δ is a small parameter that vanishes at the bifurcation point. From the switching conditions at these two times, it follows that

$$y(d - \delta) = h(d - \delta) \quad (5)$$

$$y(T + d + \delta) = h(T + d + \delta) \quad (6)$$

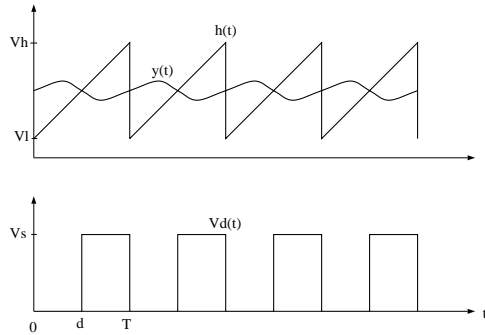


Figure 6: Waveforms of $y(t)$, $h(t)$ and $v_d(t)$ in period-one mode

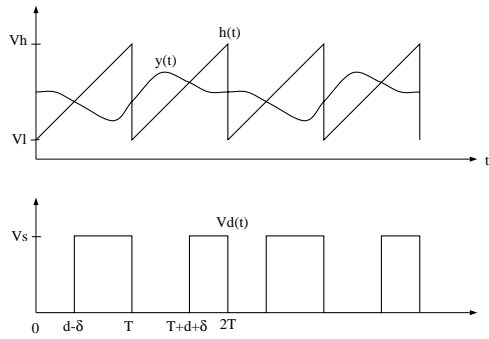


Figure 7: Waveforms of $y(t)$, $h(t)$ and $v_d(t)$ in period-two mode

The harmonic balance method is a tool that can be used to analyze periodic solutions in nonlinear systems. In the buck converter, the nonlinearity results from the switch. In the steady-state, v_d is a periodic signal and can be represented by a Fourier series. By “balancing” the equations above (written in Fourier series form) at the switching instants, a condition for existence of a periodic solution is derived.

The harmonic balance method is applied here to determine conditions for a period doubling bifurcation to occur. The basic idea is that at such a bifurcation point (shown in Fig. 8), a period-one mode and a period-two mode coalesce. By invoking conditions for the existence of each mode, the period doubling bifurcation point can be determined. In the following, the source voltage V_s will be used as the bifurcation parameter. The critical value of the bifurcation parameter, denoted by $V_{s,*}$, is determined. If a different parameter is taken as the bifurcation parameter, the approach is similar.

In the period-one mode, $v_d(t)$ is periodic with angular frequency ω_s , and can be expressed as the Fourier series

$$v_d(t) = \sum_{n=-\infty}^{\infty} c_n e^{jn\omega_s t} \quad \text{where} \quad c_n = \frac{V_s}{j2n\pi} (e^{-jn\omega_s d} - e^{-jn\omega_s T}) \quad (7)$$

Let the duty cycle be D_c . Then $D_c = 1 - d/T$. The average value of $v_d(t)$, denoted as $[v_d(t)]_{\text{AVE}}$, is

$$[v_d(t)]_{\text{AVE}} = c_0 = (1 - d/T)V_s = D_c V_s \quad (8)$$

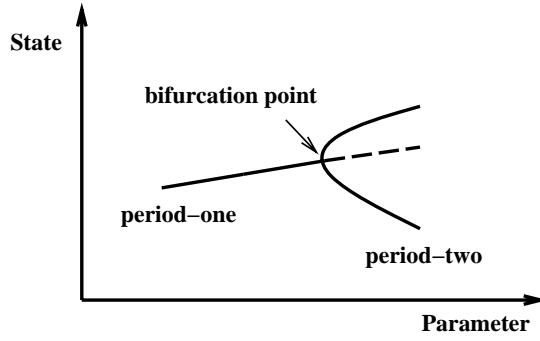


Figure 8: Period doubling bifurcation.

This agrees with the standard result from the averaging method [13].

From Fig. 2, the signal at the output of the error amplifier is

$$\begin{aligned}
 y(t) &= gV_r + \sum_{n=-\infty}^{\infty} c_n e^{jn\omega_s t} G(jn\omega_s) \\
 &= gV_r + V_s \left(\left(1 - \frac{d}{T}\right) G(0) + \left(\frac{1}{\pi}\right) \text{Im} \left(\sum_{n=1}^{\infty} \frac{e^{-jn\omega_s d} - 1}{n} e^{jn\omega_s t} G(jn\omega_s) \right) \right) \quad (9)
 \end{aligned}$$

Using Eqs. (9) and (4), V_s can be written in terms of d as

$$V_s = \frac{h(d) - gV_r}{\left(1 - \frac{d}{T}\right) G(0) + \left(\frac{1}{\pi}\right) \text{Im} \left[\sum_{n=1}^{\infty} \frac{1 - e^{jn\omega_s d}}{n} G(jn\omega_s) \right]} \quad (10)$$

Similarly, in the period-two mode, $y(t)$ is $2T$ -periodic and can be represented as the Fourier series

$$y(t) = gV_r + \sum_{n=-\infty}^{\infty} c_n e^{\frac{jn\omega_s t}{2}} G\left(\frac{jn\omega_s}{2}\right) \quad (11)$$

where

$$c_n = \begin{cases} \left(\frac{V_s}{n\pi}\right) e^{-\frac{jn\omega_s d}{2}} \sin\left(\frac{nn\omega_s \delta}{2}\right), & \text{if } n \text{ is odd} \\ \left(\frac{V_s}{jn\pi}\right) \left(e^{-\frac{jn\omega_s d}{2}} \cos\left(\frac{nn\omega_s \delta}{2}\right) - e^{-\frac{jn\omega_s T}{2}} \right), & \text{if } n \text{ is even} \end{cases}$$

Subtracting (5) from (6) and substituting (11) for y gives

$$\delta \frac{V_h - V_l}{T} =$$

$$\begin{aligned}
& \left(\frac{V_s}{\pi}\right)\text{Re}\left(-\sum_{k=1}^{\infty}\frac{1}{2k-1}G\left(j\left(k-\frac{1}{2}\right)\omega_s\right)\sin\left((2k-1)\omega_s\delta\right)\right. \\
& \left.+\sum_{k=1}^{\infty}\frac{1}{2k}G(jk\omega_s)(\sin(2k\omega_s\delta)-2e^{jk\omega_s d}\sin(k\omega_s\delta))\right)
\end{aligned} \tag{12}$$

Solving for V_s gives another expression for V_s in terms of d and δ :

$$V_s = \frac{\frac{\delta\pi(V_h-V_l)}{T}}{\text{Re}\left(-\sum_{k=1}^{\infty}\left(\frac{1}{2k-1}G\left(j\left(k-\frac{1}{2}\right)\omega_s\right)\sin\left((2k-1)\omega_s\delta\right)+\frac{1}{2k}G(jk\omega_s)(\sin(2k\omega_s\delta))-2e^{jk\omega_s d}\sin(k\omega_s\delta)\right)\right)} \tag{13}$$

Recall that δ is small and that, if a period doubling bifurcation occurs, then $\delta = 0$ at the bifurcation point. Using L'Hôpital's Rule, the critical value of V_s at the bifurcation is

$$V_{s,*} = \frac{\frac{V_h-V_l}{2}}{\text{Re}\left[-\sum_{k=1}^{\infty}G\left(j\left(k-\frac{1}{2}\right)\omega_s\right)+\left(1-e^{jk\omega_s d}\right)G(jk\omega_s)\right]} \tag{14}$$

The critical values $V_{s,*}$ and d_* can be obtained graphically by plotting Eqs. (10) and (14) on the same axes. The intersection $(V_{s,*}, d_*)$ of these graphs (if it occurs) is the period doubling bifurcation point. Indeed, a necessary and sufficient condition for a period doubling bifurcation to occur is that these graphs intersect.

Generally $G(j\omega)$ is low-pass. The denominator of (14) can be approximated by the term that involves G with the smallest argument, namely, $-\text{Re}\left[G\left(\frac{j\omega_s}{2}\right)\right]$. So a good estimate for the critical value $V_{s,*}$ is

$$\frac{\frac{V_h-V_l}{2}}{-\text{Re}\left[G\left(\frac{j\omega_s}{2}\right)\right]} \tag{15}$$

This shows how the indicated system parameters affect the period doubling bifurcation. This result also suggests that the operating range of the source voltage can be increased by increasing the magnitude of the ramp, $V_h - V_l$, or by increasing the switching frequency. Therefore, if a control scheme is designed appropriately to adjust the magnitude of the ramp, the period doubling bifurcation can be prevented. This is pursued next.

4 Feedforward Control of Buck Converter

Feedforward control (from the source voltage) has been used in DC-DC converters to obtain a faster transient response [13]. In this section, feedforward control is used to prevent period doubling bifurcation. Under certain conditions, line regulation can also be achieved. (Line regulation entails regulating the output voltage close to a constant for different values of source voltage.)

Here a feedforward control scheme is proposed to adjust the ramp signal $h(t)$ by setting $V_l = k_l V_s$ and $V_h = k_h V_s$.

4.1 Prevention of Period Doubling Bifurcation

Define the following function of d :

$$H(d) =: 2\text{Re}\left[-\sum_{k=1}^{\infty} G(j(k - \frac{1}{2})\omega_s) + (1 - e^{jk\omega_s d})G(jk\omega_s)\right] \quad (16)$$

Define $H_{max} =: \max_{0 < d < T} H(d)$ and $H_{min} =: \min_{0 < d < T} H(d)$.

The condition for bifurcation in Eq. (14) becomes

$$H(d) = k_h - k_l \quad (17)$$

If the values of k_h and k_l are chosen to satisfy $(k_h - k_l) > H_{max}$ or $(k_h - k_l) < H_{min}$, the period doubling bifurcation is prevented because the bifurcation condition is never met.

4.2 Line Regulation

In the last subsection, one has two degrees of freedom in choosing the values of k_h and k_l . This freedom can be used to achieve another objective besides preventing period doubling bifurcation. A common objective in DC-DC conversion is to achieve line regulation, which is addressed in this section.

First, an equation related to the duty cycle $D_c = 1 - d/T$ is derived. Assume the switching frequency is high enough that the high order terms in Eq. (10) can be ignored because of the

low-pass nature of $G(s)$. Then Eq. (10) becomes

$$V_s = \frac{V_l + (V_h - V_l)\frac{d}{T} - gV_r}{(1 - \frac{d}{T})G(0)} \quad (18)$$

Solving this equation for $\frac{d}{T}$ gives

$$\frac{d}{T} = \frac{G(0)V_s - V_l + gV_r}{G(0)V_s - V_l + V_h} \quad (19)$$

Next, the average output voltage, denoted as $[v_o]_{\text{AVE}}$, can be related to the source voltage V_s as

$$\begin{aligned} [v_o]_{\text{AVE}} &= [v_d]_{\text{AVE}}G_1(0) \quad (\text{from Fig. 2}) \\ &= (1 - \frac{d}{T})V_sG_1(0) \quad (\text{from Eq. (8)}) \\ &= \left(\frac{V_h - gV_r}{G(0)V_s - V_l + V_h}\right)V_sG_1(0) \quad (\text{from Eq. (19)}) \\ &= \left(\frac{k_hV_s - gV_r}{G(0) - k_l + k_h}\right)G_1(0) \quad (20) \end{aligned}$$

Setting $k_h = 0$, then the average output voltage v_o is independent of the source voltage V_s . From Eq. (20),

$$k_l = G(0) + \frac{gV_rG_1(0)}{[v_o]_{\text{AVE}}} \quad (21)$$

Thus, given a buck converter power stage ($G_1(s)$) with desired average output $[v_o]_{\text{AVE}}$, and an error amplifier (g and $G_2(s)$), line regulation can be achieved by adding a feedforward loop to adjust the ramp $h(t)$ by setting $V_h = 0$ and $V_l = k_lV_s$ with k_l as in Eq. (21).

4.3 Combined Period Doubling Prevention and Line Regulation

If $k_h = 0$ and the values of k_l given by Eq. (21) satisfy $k_l < -H_{\text{max}}$ or $k_l > -H_{\text{min}}$, both prevention of period doubling bifurcation and line regulation are achieved.

5 An Illustrative Example

Consider the controlled buck converter example from [2]. The circuit is shown in Fig. 1. The system parameters are $T = 400\mu s$, $L = 20mH$, $C = 47\mu F$, $R = 22\Omega$, and $h(t) = 3.8 + 4.4[\frac{t}{T} \bmod 1]$. The (static) dynamics of the error amplifier is $y = 8.4(v_o - V_r)$. The source voltage V_s is used as the bifurcation parameter. It has been shown that a period doubling bifurcation occurs at $V_s = 24.5$ through simulation [2] and through calculating the locus of the eigenvalues of a discrete-time model [4, 14]. The bifurcation diagram is shown in Fig. 9. From the diagram, the nominal operating range of V_s is short (16V to 24.5V). In this range of V_s , the output voltage varies from 11.9V to 12.03V as the source voltage varies.

The period doubling bifurcation point can be determined by plotting Eqs. (10) and (14) together (see Fig. 10). The intersection $(V_{s,*}, d_*)$ of these graphs is the period doubling bifurcation point.

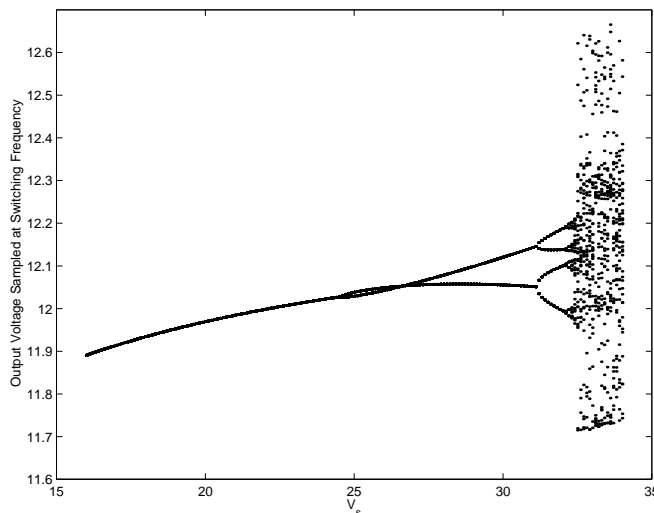


Figure 9: Bifurcation diagram of the circuit in Fig. 1

In the following, a feedforward scheme is designed and added to the original controlled buck converter to achieve (i) a wider V_s operating range (16V to 35V) without period doubling bifurcation and (ii) line regulation with $[v_o]_{AVE} = 10V$

A simplified dynamic model of the type shown in Fig. 5 can be obtained for the circuit in Fig. 9. In the resulting model, the square wave generator will be as shown in Fig. 2; the gain $g = -8.4$;

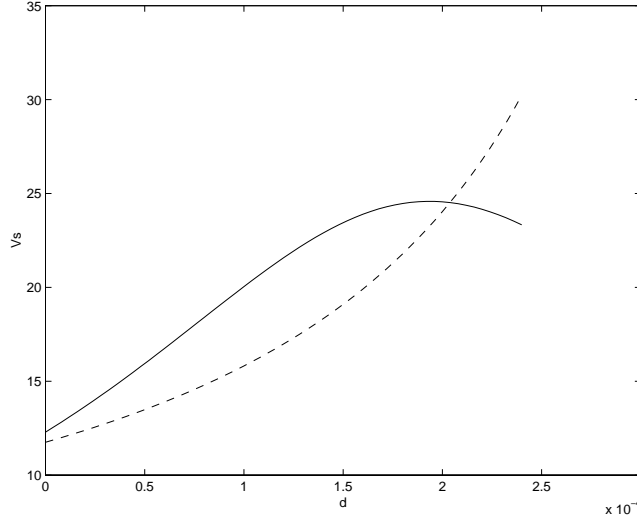


Figure 10: Plot of Eq. (10) (dashed line) and Eq. (14) (solid line). The intersection determines the period doubling bifurcation point

and the transfer function

$$G(s) = G_1(s)G_2(s) = \frac{8.4}{LCs^2 + \frac{L}{R}s + 1} \quad (22)$$

A plot of $H(d)$ is obtained using Eq. (16), and is shown in Fig. 11 (here, $H_{max} = 0.358$ and $H_{min} = 0.1792$). Let $k_h = 0$. From Eq. (21), $k_l = -1.092$. The condition $k_l < -H_{max}$ is satisfied. Thus both prevention of period doubling bifurcation and line regulation can be achieved.

In feedforward control, the ramp signal has $V_l = 0$, and V_h is adjusted according to the value of V_s according to $V_h = -1.092V_s$. The resulting bifurcation diagram of the buck converter with the feedforward control is shown in Fig. 12. The figure shows a wider operating range for V_s (16V to 35V) and good line regulation, with $[v_o]_{AVE} = 10V$.

Take $V_s = 28V$ for example. The output voltage response of the circuit in Fig. 1 with feedforward control during start-up (starting from $(i_L, v_o) = (0, 0)$) is shown in Fig. 13. The output voltage is regulated to 10V. The switching operation depends on intersection of the signals $h(t)$ and $y(t)$. These are shown in Fig. 14. The signal $h(t)$ is negative, this is different from the traditional positive ramp.

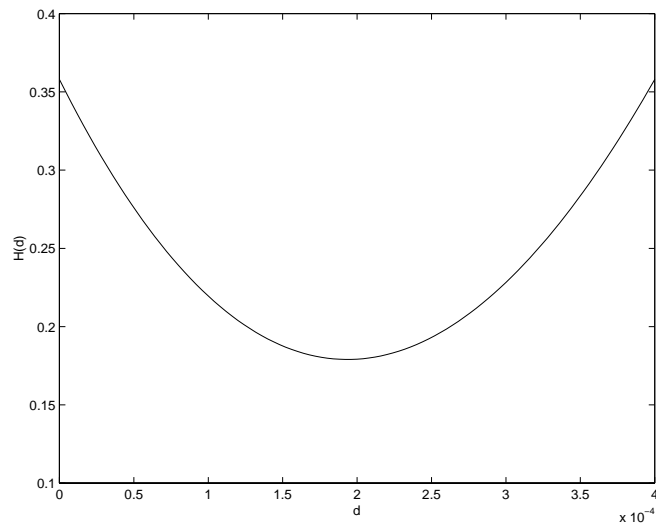


Figure 11: Plot of function $H(d)$

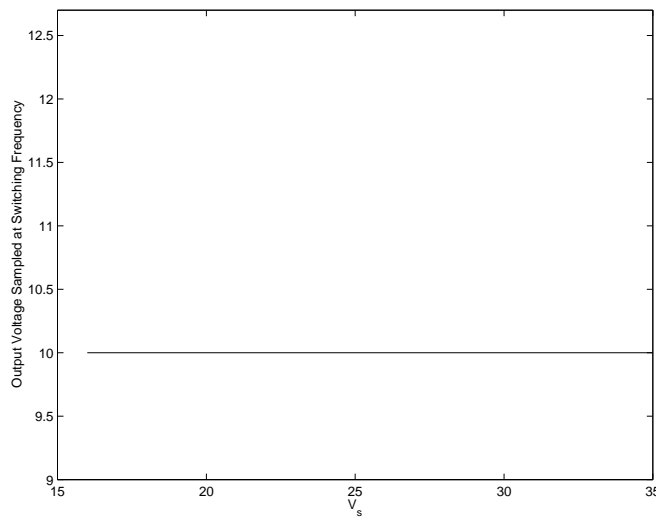


Figure 12: Bifurcation diagram of the circuit in Fig. 1 with feedforward control

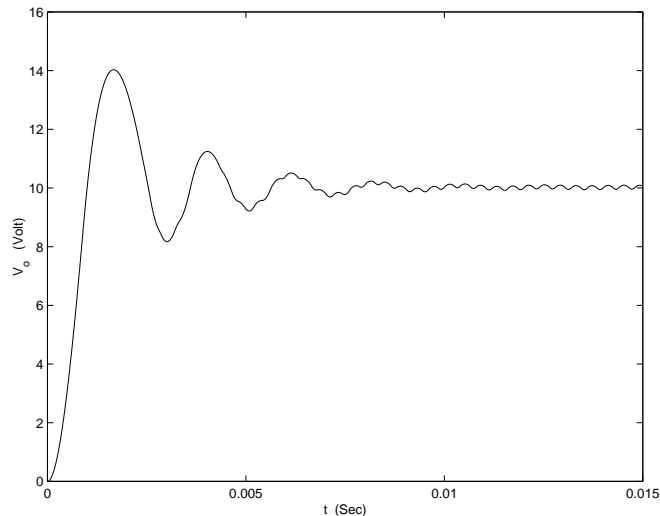


Figure 13: Output voltage response of the circuit in Fig. 1 with feedforward control during start-up

6 Concluding Remarks

Harmonic balance analysis of period doubling bifurcation in the buck converter in continuous conduction mode has been performed. A simple dynamic model of the buck converter in voltage mode or current mode control has been derived. This model consists of the feedback connection of a linear system and a nonlinear one. A condition for period doubling bifurcation was given in terms of the solvability of a pair of algebraic equations. Based on this condition, a feedforward control scheme was used to adjust the compensating ramp, stabilizing the buck converter. A wider operating range for the source voltage was achieved, along with output voltage regulation. Simulations were used to illustrate the effectiveness of the design technique.

Acknowledgments

This research has been supported in part by the the Office of Naval Research under Multidisciplinary University Research Initiative (MURI) Grant N00014-96-1-1123, and by the U.S. Air Force Office of Scientific Research under Grant F49620-96-1-0161.

References

- [1] J.H.B. Deane and D.C. Hamill, "Instability, subharmonics, and chaos in power electronics circuits," *IEEE Transactions on Power Electronics*, vol. 5, no. 3, pp. 260–268, 1990.

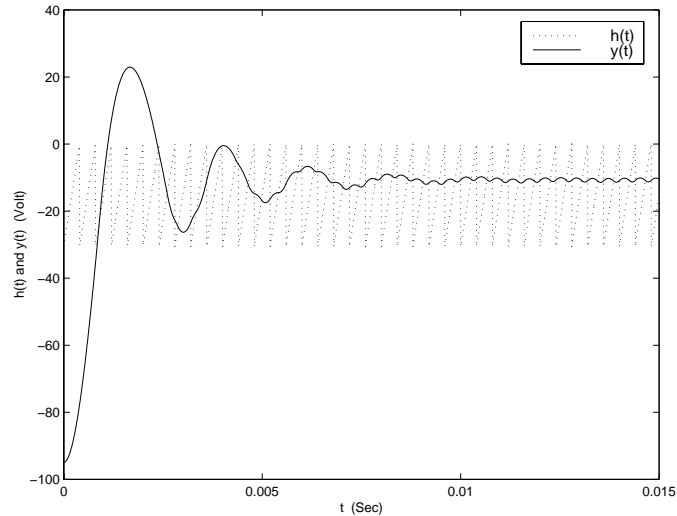


Figure 14: Waveforms of $h(t)$ and $y(t)$ of the circuit in Fig. 1 with feedforward control during start-up

- [2] D.C. Hamill, J.H.B. Deane, and J. Jefferies, “Modeling of chaotic DC-DC converters by iterated nonlinear mappings,” *IEEE Transactions on Power Electronics*, vol. 7, no. 1, pp. 25–36, 1992.
- [3] C.K. Tse, “Flip bifurcation and chaos in three-state boost switching regulators,” *IEEE Transactions on Circuits and Systems-I: Fundamental Theory and Applications*, vol. 41, no. 1, pp. 16–23, 1994.
- [4] E. Fossas and G. Olivar, “Study of chaos in the buck converter,” *IEEE Transactions on Circuits and Systems-I: Fundamental Theory and Applications*, vol. 43, no. 1, pp. 13–25, 1996.
- [5] G. Podder, K. Chakrabarty, and S. Banerjee, “Experimental control of chaotic behavior of buck converter,” *IEEE Transactions on Circuits and Systems-I: Fundamental Theory and Applications*, vol. 42, no. 8, pp. 100–101, 1995.
- [6] G. Poddar, K. Chakrabarty, and S. Banerjee, “Control of chaos in DC-DC converters,” *IEEE Transactions on Circuits and Systems-I: Fundamental Theory and Applications*, vol. 45, no. 6, pp. 672–676, 1998.
- [7] R.D. Middlebrook and S. Ćuk, “A general unified approach to modelling switching-converter power stages,” in *IEEE Power Electronics Specialists Conf. Rec.*, 1976, pp. 18–34.
- [8] R. Genesio and A. Tesi, “Harmonic balance methods for the analysis of chaotic dynamics in nonlinear systems,” *Automatica*, vol. 28, no. 3, pp. 531–548, 1992.
- [9] C. Piccardi, “Bifurcations of limit cycles in periodically forced nonlinear systems: the harmonic balance approach,” *IEEE Transactions on Circuits and Systems-I: Fundamental Theory and Applications*, vol. 41, no. 4, pp. 315–320, 1994.

- [10] A. Tesi, E.H. Abed, R. Genesio, and H.O. Wang, "Harmonic balance analysis of period-doubling bifurcations with implications for control of nonlinear dynamics," *Automatica*, vol. 32, no. 9, pp. 1255–1271, 1996.
- [11] E. X.-Q. Yang, *Extended Describing Function Method for Small-Signal Modeling of Resonant and Multi-Resonant Converters*, Ph.D. thesis, Virginia Polytechnic Institute and State University, 1994.
- [12] J.O. Groves Jr., *Small Signal Analysis of Nonlinear Systems with Periodic Operating Trajectories*, Ph.D. thesis, Virginia Polytechnic Institute and State University, 1995.
- [13] N. Mohan, T.M. Undeland, and W.P. Robbins, *Power Electronics: Converters, Applications, and Design*, Wiley, New York, 1995.
- [14] C.-C. Fang, *Sampled-Data Analysis and Control of DC-DC Switching Converters*, Ph.D. thesis, University of Maryland, College Park, 1997.